Biomedicine & Pharmacotherapy 162 (2023) 114679

Contents lists available at ScienceDirect

Biomedicine & Pharmacotherapy

journal homepage: www.elsevier.com/locate/biopha

Exploiting bioactive natural products of marine origin: Evaluation of the meroterpenoid metachromin V as a novel potential therapeutic drug for colorectal cancer

Donatella Lucchetti [a,b,1], Francesca Luongo [b,1], Filomena Colella [a,1], Enrico Gurreri [b], Giulia Artemi [a], Claudia Desiderio [d], Stefano Serra [e], Felice Giuliante [f], Ruggero De Maria [a,b], Alessandro Sgambato [a,b,*], Alberto Vitali [d], Micol Eleonora Fiori [c]

[a] Dipartimento di Medicina e Chirurgia traslazionale - Facoltà di Medicina e Chirurgia, Università Cattolica del Sacro Cuore, Rome, Italy
[b] Fondazione Policlinico Universitario "A. Gemelli" - IRCCS, Rome, Italy
[c] Department of Oncology and Molecular Medicine, Istituto Superiore di Sanità, Rome, Italy
[d] Istituto di Scienze e Tecnologie Chimiche"Giulio Natta" (SCITEC), Consiglio Nazionale delle Ricerche (CNR), Rome, Italy
[e] Istituto di Scienze e Tecnologie Chimiche "Giulio Natta" (SCITEC), Consiglio Nazionale delle Ricerche (CNR),. Milano, Italy
[f] Dipartimento di Scienze Mediche e Chirurgiche, Chirurgia Generale ed Epato-Biliare, Fondazione Policlinico Universitario "A. Gemelli= - IRCCS, Rome, Italy

ARTICLE INFO

Keywords:
Natural products
Therapeutic drug
Colorectal cancer
Cancer stem cells

ABSTRACT

Colorectal cancer (CRC) is the second most common cause of cancer death, leading to almost 1 million deaths per year. Despite constant progress in surgical and therapeutic protocols, the 5-year survival rate of advanced CRC patients remains extremely poor. Colorectal Cancer Stem Cells (CRC-CSCs) are endowed with unique stemness-related properties responsible for resistance, relapse and metastasis. The development of novel therapeutics able to tackle CSCs while avoiding undesired toxicity is a major need for cancer treatment. Natural products are a large reservoir of unexplored compounds with possible anticancer bioactivity, sustainability, and safety. The family of meroterpenoids derived from sponges share interesting bioactive properties. Bioassay-guided fractionation of a meroterpenoids extract led to the isolation of three compounds, all cytotoxic against several cancer cell lines: Metachromins U, V and W. In this study, we evaluated the anticancer potential of the most active one, Metachromins V (MV), on patient-derived CRC-CSCs. MV strongly impairs CSCs-viability regardless their mutational background and the cytotoxic effect is maintained on therapy-resistant metastatic CSCs. MV affects cell cycle progression, inducing a block in G2 phase in all the cell lines tested and more pronouncedly in CRC-CSCs. Moreover, MV triggers an important reorganization of the cytoskeleton and a strong reduction of Rho GTPases expression, impairing CRC-CSCs motility and invasion ability. By Proteomic analysis identified a potential molecular target of MV: CCAR1, that regulates apoptosis under chemotherapy treatments and affect β-catenin pathway. Further studies will be needed to confirm and validate these data in in vivo experimental models

1. Introduction

Approximately 11 % of all annually diagnosed cancers and cancer-related deaths worldwide is due to colorectal cancer (CRC). CRC is third in terms of incidence and second for mortality worldwide [1]. At initial stages, surgical resection and chemotherapy are the most effective treatments for CRC patients. For metastatic CRC (mCRC), surgical resection is the best therapeutic option with curative intents, often coupled with peri-operative treatment based on cytotoxic chemotherapy and biological drugs [2]. However, the 5-year survival rate of advanced CRC patients (stage III-IV) remains extremely poor. Notwithstanding significant advances in anticancer therapy in the last decades, the development of resistance to antineoplastic drugs and their lack of specificity leading to toxic side effects still represent a major cause of therapeutic failure and (eventually) death [3]. Notably, a subpopulation of CRC cells, named Colorectal Cancer Stem Cells (CRC-CSCs) has been

* Corresponding author at: Dipartimento di Medicina e Chirurgia traslazionale - Facoltà di Medicina e Chirurgia, Università Cattolica del Sacro Cuore, Rome, Italy.
E-mail address: alessandro.sgambato@unicatt.it (A. Sgambato).
[1] Co-first authors

https://doi.org/10.1016/j.biopha.2023.114679
Received 15 February 2023; Received in revised form 26 March 2023; Accepted 6 April 2023
Available online 15 April 2023

identified as the main responsible for resistance, relapse and metastasis, due to their unique stemness-related properties [4]. The development of novel therapeutics able to tackle CSCs-based resistance while avoiding undesired toxicity on healthy tissues is a major unmet need in cancer research.

Tumor preventive capacities have been recognized for several natural compounds, leading to the interesting hypothesis that natural, non-toxic molecules may constitute a weapon in the battle against cancer. The natural products (NPs) are a large reservoir of unexplored compounds with possible anticancer bioactivity, sustainability, and safety [5]. Besides the huge number of NPs derived from terrestrial plants, an even more growing number of bioactive compounds is being isolated and characterized from the marine environment. Indeed, of the 1211 small-molecule drugs approved between 1981 and 2014, 6 % were unaltered NPs and 26 % were NPs derivatives. The sea is still an undiscovered world especially in the field of medicinal chemistry and bioactive compounds, and this is very intriguing considering that the 70% of the world is indeed undersea [6]. Among the various sea life forms, sponges represent one of the most promising and prolific sources of interesting NPs [7,8]. The great variety of bioactive molecules produced by sponges is mainly due to their particular sessile form of life resembling in this terrestrial plants. Regarding the anticancer properties, different organic compounds have been isolated from sponges exerting distinct mechanisms of action as pro-apoptotic [9], anti-proliferative, diminution of chemoresistance [10] and cytoprotective effects on non-tumoral cells treated with cytotoxic anticancer drugs [11].

An interesting group of bioactive compounds is represented by the family of the meroterpenoids whose mixed biosynthetic origin is from the polyketide and isoprenoid pathways. These compounds, isolated from different sources, include both primary (plastoquinones, vitamins, ubiquinones) and secondary (terpenyl-quinones/hydroquinones) metabolites, representing important molecules for the physiology of the cell [12]. Meroterpenoids are terpenoid–polyketide NPs characterized by a variety of biological activities. The chemical structure of 1,4-hydroquinone meroterpenoid is common to many NPs. These compounds occur in living beings very different from each other such as higher plants, sponges, ascidians and mushrooms. Since 1,4-hydroquinones are of a mixed biogenetic origin, the structure of the isoprenic moiety may change considerably depending upon the natural sources of 1,4-hydroquinone meroterpenoid. Particularly, an extract of the sponge *Thorecta reticulata* has showed a significant cytotoxicity in SF-268, MCF-7, H460, HT-29 and CHO-K1 cells [13]. Bioassay-guided fractionation of a meroterpenoids extract of the sponge led to the isolation of three compounds, Metachromins U, V and W, found to be cytotoxic against all cancer cell lines tested, with Metachromin V being the most active one [14]. The chemical structure of Metachromin V was unambiguously determined through extensive NMR analysis. Differently, the enantiomeric composition of Metachromin V in the sponge extracts was not investigated as its measured optical rotation value was null, thus pointing to the occurrence of the natural compound in racemic form.

Drug chirality has long attracted the attention of Food and Drug Administration (FDA) and European Medicines Agency (EMA) that developed specific regulations, with the current tendency moving towards the development of enantiopure medicines by *de novo* synthesis and/or the practice of chiral switch for commercially available racemic drugs [15]. The chirality of pharmacologically active compounds is important in drug research since enantiomers usually exhibit different pharmacokinetic and pharmacological profiles, the distomer possibly exhibiting, in addition to its absent or reduced activity, important toxic effects. This has led to the need to ensure processes of stereoselective synthesis and the availability of chiral analytical methods for the separation and quantification of the enantiomers [16,17]. Therefore studies on novel therapeutics needs to improve efficacy and/or safety for chiral compounds by separately testing their enantiomeric forms.

Recently, we successfully prepared the Metachromin V (*S*)-enantiomer (S-MV) through a new stereoselective synthetic approach [14]. The aforementioned study, beside confirming the chemical structure of the natural compound, allowed the unambiguous assignation of the (*S*)-configuration to the dextrorotatory isomer. In addition, the described synthetic procedure gave a reliable access to S-MV, in high stereoisomeric purity,starting from commercially available precursors. The aim of the present study was the evaluation of the anticancer activity of MV. Therefore, we decided to investigate the biological activity of the MV stereoisomeric form available in higher enantiomeric purity, namely the (*S*)-isomer. We report here the study of the S-MV anticancer activity in a panel of colorectal cancer stem cells (CRC-CSCs), isolated from primary tumor or from liver metastases.

2. Materials and methods

2.1. Isolation and propagation of CR-CSCs

The purification and culture of CSphCs, from primary tumor specimens and liver metastases of patients diagnosed with CRC, were performed as already described in Ricci Vitian et al. [4], in accordance with the ethical standards of Human Experimentation (authorization AIRC IG 2015, 17621, 2016, Fondazione Policlinico A Gemelli IRCCS, Rome, Italy). Briefly, specimens were digested in DMEM medium supplemented with 1.5 mg/mL of collagenase (Thermo Fisher) for 10–15 min at 37 °C, thoroughly washed with PBS (Phosphate buffered saline), filtered with 100 μm cell strainer, resuspended in serum-free stem cell medium and cultured in ultra-low adhesion flasks. The authentication of CR-CSphCs was routinely performed by the short tandem repeat (STR) DNA profiling kit (GlobalFiler™ STR kit, Applied Biosystem, Thermo Fisher Scientific, Waltham, MA, USA) followed by sequencing analysis on ABIPRISM 3130 (Applied Biosystem, Thermo Fisher Scientific Waltham, MA, USA). Cell cultures were monitored for the presence of mycoplasma on a regular basis. All CRC-SCs were validated for their capability to generate neoplasms faithfully phenocopying the original patient tumor when xenotransplanted into immunocompromised mice.

Serum Free Stem Cell medium: Advanced DMEM F12 (ADF) added with 100 units/mL of penicillin, 100 μg/mL of streptomycin, 0.29 mg/mL glutamine, 6 g/L glucose, 5 mM HEPES, 3.6 g/L BSA, 0.1 % NaHCO3, 4 mg/L (≥700 U/L) heparin,10 mM nicotinamide, 1 g/L apo-transferrin, 250 mg/L insulin, 161 mg/L putrescine, 52 μg/L sodium selenite, 62 μg/L progesterone, 10 mM HEPES, 20 ng/mL human recombinant EGF, 10 ng/mL human recombinant bFGF.

2.2. Metachromin treatment for dose response curves and histograms

For dose response curves, CSCs and metastatic CSCs (met-CSCs) were dissociated with TrypLETM (Gibco,Thermo Fisher Scientific) and living cells were counted with trypan blue. Cells were seeded in a 96-well plate, 5000 cells per well in 80ul. After 24 h to allow the restoration of cells, CSCs and met-CSCs were treated with S-MV diluted in 20 μL of medium at growing doses spanning between 2,5 and 20 μM (dilution rate 1:2). DMSO (Metachromin's solvent) at 0,25 % was used as control.

For combinatorial treatment of S-MV and chemotherapy, met-CSCs were treated with 10 μM of 5-Fluoruracil (5-FU) and Oxaliplatin (Selleck Chemicals) in combination. 5-FU was added to culture medium two hours after Oxaliplatin [18].

Cell viability was measured by Cell-titer Glo (Promega) at t = 0 (24 h after seeding, before treatment) and t = 72 h, following manufacturer's instructions. Briefly, Cell Titer-Glo Reagent was added on the cells in each well, the plate was incubated at 37 °C for 10 min, shaking to mix the components, allow cell lysis and stabilize the luminescent signal. Finally, the light signal was measured at the luminometer (Beckman Coulter DTX 880 Multimode Detector). Viability data were elaborated with GraphPad Prism v8.

2.3. Migration assay

For the migration assay, 1×10^3 cells pre-treated with different concentrations of S-MV for 24 h were plated in triplicate in the upper chambers of a Fluoroblok plate (BD Biosciences, 351164) and treated again at the same concentrations. The lower chambers were filled with fresh medium. Plates were incubated at 37 °C for 24 h, then cells were stained with 50 μM Calcein AM (Sigma) for 30 min and analyzed by fluorescence microscope. Quantitative image analysis was performed by ImageJ software.

2.4. Cell cycle analysis

For cell cycle analysis, 1×10^6 cells treated with different S-MV concentrations (0–1 - 2,5–5 μM) for 24 h were dissociated and filtered using Cell Strainer (EASYstrainer 70 μm, Greiner bio-one). Cells were resuspended in Nicoletti's Buffer containing 0.1 % sodium citrate, 9.65 mM NaCl, 0.1 % NP40 Cell Lysis buffer and 1 μg/mL propidium iodide (Sigma-Aldrich). After 30 min incubation on ice, protected from light, samples were analyzed by a CytoFLEX S, Beckman Coulter, Milan, Italy).

2.5. Cell apoptosis

For cell apoptosis analysis, 1×10^6 cells treated with different Metachromin concentration (1–5 μM) for 48 h and 72 h were dissociated and filtered using Cell Strainer (EASYstrainer 70 μm, Greiner bio-one), then samples were collected and stained with the Annexin-V-FLUOS Staining Kit to evaluate the number of apoptotic cells, according to the manufacturer's instructions (REF:11858777001 Roche, Mannheim, Germany). After 15 min incubation at RT, samples were analyzed by CytoFLEX S, Beckman Coulter, Milan, Italy).

2.6. Western blot analysis

The cells were lysed using a lysis buffer (50 mM Tris-HCl pH 7.2, 5 mM $MgCl_2$, 50 mM NaCl, 0.25 %, 0.1 % SDS, and 1 % Triton X-100) containing protease inhibitors (2 mM phenyl methyl sulfonyl fluoride, 10 mg/mL aprotinin, and 2 mM Na_3VO_4, 100 mM NaF). Protein concentration was assessed using the Bradford method (Bradford protein assay kit II, Bio-Rad, Hercules, CA, USA), with BSA used as a standard. Cell lysates (40 μg) were resolved by SDS PAGE (Sodium Dodecyl Sulfate PolyAcrylamide Gel Electrophoresis) 10% under reducing conditions and were transferred to PVDF blotting membranes (GE Healthcare, Solingen, Germany) and analyzed using the enhanced chemiluminescence kit for Western blotting detection (Advansta, WesternBright TM ECL, Bering Drive San Jose, CA, USA). Primary antibodies were used following suppliers' instructions and included the following: mouse monoclonal anti-human PARP-1 (N-20; sc-1561; dilution 1:500; Santa Cruz Biotechnology, Inc.), rabbit monoclonal anti-human p21 (Waf1/Cip1 (12D1); #2947; dilution 1:1000; Cell Signaling Technology, cst), rabbit monoclonal anti-human cleaved-caspase 3 (Asp175(5A1E); #9664; dilution 1:1000; Cell Signaling Technology, cst); rabbit monoclonal anti-human caspase 9 (#9502; dilution 1:1000; Cell Signaling Technology, cst); rabbit monoclonal anti-human Sox2(D6D9 XP®; #3579; dilution 1:1000; Cell Signaling Technology, cst); mouse monoclonal anti-human β-Actin (C4; sc-47778; dilution 1:500; Santa Cruz Biotechnology, Inc.), rabbit polyclonal anti-human β-catenin (#9562; dilution 1:1000; Cell Signaling Technology, cst); mouse monoclonal anti-human cyclin D1 (72–13G; sc-450; dilution 1:200; Santa Cruz Biotechnology, Inc.), mouse monoclonal anti-human cyclin B1 (D-11; sc-7393; dilution 1:200; Santa Cruz Biotechnology, Inc.), mouse monoclonal anti-human CD133 (AC133; W6B3cdilution, 1:200; Miltenyi Biotec S.r.l.); rabbit polyclonal anti-human p44/42 MAPK (Erk1/2) (#9101; dilution 1:1000; Cell Signaling Technology, cst); rabbit polyclonal anti-human phospho p44/42 MAPK (Erk1/2) (#9102; dilution 1:1000; Cell Signaling Technology, cst); rabbit polyclonal anti-human CCAR1 (A300–435A-T; dilution 1:1000, Bethyl Laboratories, Inc.), mouse monoclonal anti-human CDC43 ((B-8); sc-8401; dilution 1:200; Santa Cruz Biotechnology, Inc.), mouse monoclonal anti-human RhoA (26C4; sc-418; dilution 1:200; Santa Cruz Biotechnology, Inc.), mouse monoclonal anti-human Rac 1 (C-14; sc-217; dilution 1:200; Santa Cruz Biotechnology, Inc.), mouse monoclonal anti-human C-Myc (9E10; sc-40; dilution 1:200; Santa Cruz Biotechnology, Inc.), mouse monoclonal anti-human p-Akt1/2/3 (C-11; sc-514032; dilution 1:200; Santa Cruz Biotechnology, Inc.), mouse monoclonal anti-human Akt1 (5G12; sc-81435; dilution 1:200; Santa Cruz Biotechnology, Inc.), mouse monoclonal anti-human Nanog (H-2; sc-374103; dilution 1:200; Santa Cruz Biotechnology, Inc.).

2.7. Colony-forming efficiency

For colony-forming efficiency assay, 250 HT29 or CaCo2 cells were plated onto 60-mm culture dishes in Dulbecco's modified Eagle's medium supplemented with 10 % fetal bovine serum, 1 % penicillin-streptomycin, and 2 mM L-glutamine at 37 °C, in a humid 5 % CO_2 atmosphere for HT29 cell line and Dulbecco's modified Eagle's medium supplemented with 20% fetal bovine serum, 1 % penicillin-streptomycin, and 2 mM L-glutamine at 37 °C, in a humid 5 % CO_2 atmosphere for CaCo2 cell line. After 2 weeks, the colonies were fixed with of 10 % methanol and 10 % acetic acid, stained with crystal violet 0,01 %, and counted.

2.8. Confocal microscopy

5×10^4 HT29 cells for well were plated onto chambered coverslip with 8 individual wells, incubated for 24 h and treated with different Metachromin concentrations (0–1 - 7.5–15 μM) for 3 h, 6 h and 9 h. After treatment, wells were washed with PBS and fixed with paraformaldehyde (PFA, polymeric formaldehyde) 0,01 % for 30 min. Then, wells were washed and the cells were permeabilized with Triton 1 %. Afterwards, cells were stained with fluorescein isothiocyanate–labeled phalloidin for 45 min. Subsequently, the slides were mounted with DAPI (Fluoroshield™ with DAPI; Sigma-Aldrich) and analyzed by fluorescence microscope. Images were taken using ImageJ software version 1.41 (NIH, Bethesda, Rockville, MD, USA). Analyses were performed using the OrientationJ plugins to analyze the coherency.

2.9. ECIS system

An electric cell-substrate impedance sensing (ECIS) system (Applied Bio-Physics Inc., Troy, NY, USA) was used to monitor real-time cell growth and motility. Briefly, an 8 wells array containing gold electrodes (Applied Biophysics 8W10E; Linea SisLab, Milan, Italy) was coated with 10 mM cysteine (200 μL/well) for 15 min, followed by aspiration. Then, the array was incubated with medium (200 μL /well). Next, 2×10^5 HT29 cells for well were seeded in 400 μL of medium and treated with different S-MV concentrations (0–1 - 7.5–15 μM). Impedance, which is affected by the number and the morphology of cells covering the electrode, was monitored for a maximum of 48 h.

2.10. Cell viability assay

Cell viability was evaluated by using an MTT assay. The yellow MTT day can be reduced to purple formazan crystals by metabolically active cells. Briefly, 1×10^4 cells were plated in 100 μL of medium in 96-well microtiter plates and incubated for 24 h. Next, cells were treated with different S-MV concentrations (0–1 - 7.5–15 μM) for 48 h. MTT solution was added to each well and incubated at 37 °C for an hour and a half. The media was removed and formazan crystals were dissolved in 100 μL 0.04 N HCl/isopropanol for each well in agitation for 20 min. The amount of MTT formazan product was determined by measuring absorbance with a microplate reader at a test wavelength of 570 nm and

a reference wavelength of 630 nm.

2.11. Proteomic analysis

HT-29 and CaCo2 cells were pooled after S-MV treatment and lysed with a 0.1 M Tris-HCl, pH 8.5, 8 M Urea (Urea Buffer, UB). The obtained samples were submitted to a Filter-Assisted Sample Preparation (FASP) procedure to be further analyzed by LC/MS. The lysates were transferred in a Microcon-10 filtration device equipped with a Ultracel 10 kDa MW cut-off filter (Merck Millipore, Carrigtwohill, Irl) and centrifuged at 14,000 rpm for 15 min. The supernatant was then treated with DTT 8 mM in UB to break disulfide bonds and incubated at 37 °C for 15 min. Samples were centrifuged at 14,000 rpm for 15 min. DTT residues were removed by UB washings and subsequent centrifugation. Free thiol groups were carboxymethylated following treatment with 50 mM iodoacetamide (IAA) UB solution and incubation in the dark at room temperature (RT) for 15 min followed by centrifugation at 14,000 rpm for 15 min. Residual IAA was removed by incubating the sample with a DTT solution at 37 °C for 15 min. Samples were then digested overnight at 37 °C adding for each sample 3 μL of a 1 μg/μL trypsin (Trypsin Gold-Mass Spec Grade, PROMEGA ITALIA S.r.l, Milan, Italy) solution in 1:100 (v/v) 50 mM ammonium bicarbonate buffer. The enzymatic digestion was stopped by adding FA for a final 1 % concentration. The obtained peptides were collected by centrifugation at 14,000 rpm for 15 min, lyophilized, and redissolved in 0.1 % FA for LC-MS analysis [19].

LC-ESI-MS/MS analyses after FASP treatment were performed in triplicates for each sample on UltiMate 3000 RSLCnano System coupled to Orbitrap Elite MS detector with EASY-Spray nanoESI source (Thermo Fisher Scientific, Waltham, MA, USA) and Thermo Xcalibur 2.2 computer program (Thermo Fisher Scientific) for instrumental operation and data acquisition. EASY-Spray columns 15 cm in length × 50 μm of internal diameter (ID) were used, and PepMap C18 (2 μm particles, 100 Å pore size) (Thermo Fisher Scientific) was used for shot-gun analyses hyphenated with Acclaim PepMap100 nano-trap cartridge (C18, 5 μm, 100 Å, 300 μm i.d. × 5 mm) (Thermo Fisher Scientific) operating pre-separation peptide trapping and concentration. Chromatographic separations were performed at 40 °C in gradient elution using 0.1 % FA as eluent A and an ACN/FA solution (99.9:0.1, v/v) as eluent B as following: (i) 5 % B (7 min), (ii) from 5 % to 35 % B (120 min), (iii) from 35 % B to 99 % (15 min), (iv) 99 % B (10 min), (v) from 99 % to 5 % B (2 min), (vi) 5 % B (13 min). The mobile phase flow rate was 0.3 μL/min. The injection volume was 5 μL. The Orbitrap Elite instrument was operating in positive ionization mode at a 60,000 full scan resolution in 350–2000 m/z acquisition range, performing MS/MS fragmentation by collision-induced dissociation (CID, 35 % normalized collision energy) of the 20 most intense signals of each MS spectrum in Data-Dependent Scan (DDS) mode. The minimum signal was set to 500.0, the isolation width to 2 m/z and the default charge state to + 2. MS/MS spectra acquisition was performed in the linear ion trap at normal scan rate.

LC-MS raw data have been analyzed for protein identification by Proteome Discoverer software (version 1.4.1.14, Thermo Fisher Scientific) against the Swiss-Prot Homo sapiens proteome database (UniProtKb, Swissprot, homo+sapiens released in March 2018). The protein identification results were filtered, according to the Human Proteome Project (HPP) recommendations [20], for high confidence, minimum of 2 peptides per protein, minimum peptide length 9 amino acids and peptide rank 1. Gene ontology (GO) analysis and classification was performed by Protein Analysis Through Evolutionary Relationships (PANTHER, http://www.pantherdb.org, version 17 released 2022–02–22) tool [21] using Fisher's Exact test type with false discovery rate (FDR) correction. Functional protein interaction networks were analyzed by STRING tool (https://string-db.org) [22]. Sample data grouping analysis was performed by Venn diagram tool (Venny. An interactive tool for comparing lists with Venn's diagrams, https://bioinfogp.cnb.csic.es/tools/venny/index.html). Human Protein Atlas was the database of reference for the Cancer related classified proteins [23] (https://www.proteinatlas.org/search/protein_class:Cancer-related+genes).

3. Results

3.1. S-MV inhibits proliferation and induces apoptosis of CRC-CSCs and immortalized cancer cell lines (iCCL)

S-MV was previously shown to affect the viability of established cancer cell lines (SF-268, MCF-7, H460, HT29 and CHO-K1) with an IC_{50} ranging from 2.1 to 10 μM [13]. Here, we selected three immortalized CRC cell lines (HCT116, HT29 and CaCo2) and seven (from C_1 to C_7) primary CRC-CSCs characterized for the mutational status of recurrently CRC-altered genes (C_1 and C_2: KRAS wt and BRAF wt; C_3, C_7 and C_4: Kras mut and BRAF wt; C_5 and C_6: Kras wt and BRAF mut). We first tested the impact on cell viability of growing doses of S-MV, by Cell Titer GLo assay (Promega). We adopted the following concentrations for dose-response curves: 1.25–2.5–5–10–20 μM for HCT116, HT29 and CaCo2 (iCCL) and 0.4–1–2.5–5 μM for CRC-CSCs (Fig. 1a-b-c; Supp. Fig. 3). Our results showed that S-MV significantly reduces cell viability in both immortalized and primary CRC-CSCs cell lines, independently from KRAS and BRAF mutational status. Interestingly, CRC-CSCs displayed higher sensitivity to S-MV compared to immortalized cancer cells, as shown by the lower mean IC_{50} doses (IC_{50} 48 h= 3,5 vs 6,9; IC_{50} 72 h= 3,2 vs 7.0; p = 0,05) (Fig. 1c).

A deeper analysis revealed that S-MV strongly affected cell cycle progression, in a dose dependent manner, causing a reduction of cells in the G1/S and a substantial increase in the G2 cell cycle phases, along with accumulation of the sub-G0 fraction, indicative of apoptosis (Fig. 1d). The block in G2 phase was confirmed also in iCCL cells, while apoptosis induction was less pronounced, consistently with the observed higher sensitivity of CRC-CSCs (supp. Fig. 1a).

3.2. S-MV modulates the expression of master regulators of cell cycle in CRC-CSCs

To get further insights about the molecular mechanisms of action of S-MV on CRC-CSCs proliferation and cycle progression, we analyzed by western blot the expression of cell cycle regulatory proteins. Total protein extracts were prepared from cells exposed to growing doses of S-MV (0.4–1–2.5–5 μM) for 48 h and were analyzed to evaluate the expression levels of cyclins B1 and D1, the CDK inhibitor p21Waf1, all important regulators of cell cycle progression in mammalian cells. Moreover, we analyzed the expression of Parp-1, Caspase-3 and Caspase-9, involved in the activation of programmed cell death. As shown in Fig. 1e, the expression of both cyclins B1 and D1 was reduced by S-MV in both CRC-CSCs tested, thus confirming the flow cytometry observations (Fig. 1e; Supp. Fig. 1a). Consistent with the cell cycle arrest was also the increased expression of the cell cycle inhibitory proteins, p21Waf1 and cleaved Parp-1 detected in both cell lines. The anti-Caspase 3 and Caspase 9 antibodies used were able to detect only the active subunit generated by cleavage of the pro-caspases 3 and 9. We observed the increase of cleaved subunit of Caspase 3 and 9 in both CRC-CSCs cell lines tested (Fig. 1e; Supp. Fig. 1a).

3.3. Proteomic analysis on colon cancer cells treated with S-MV

Proteomic analysis was performed to investigate the alterations of the protein phenotype of HT29 and CaCo2 cells under treatment with S-MV to investigate its potential targets. The resulting data lists were then grouped by Venn diagram elaborations to disclose the protein elements commonly modulated by treatment in both cell lines and conditions studied, considering the data obtained in triplicate LC-MS analysis of biological triplicates, with respect to untreated cells. The workflow of proteomic data analysis is showed in Fig. 2a. The proteomic analysis of untreated HT29 and CaCo2 cells (CTRL) identified with confidence 1135 and 1200 proteins, respectively, with 946 elements in common between

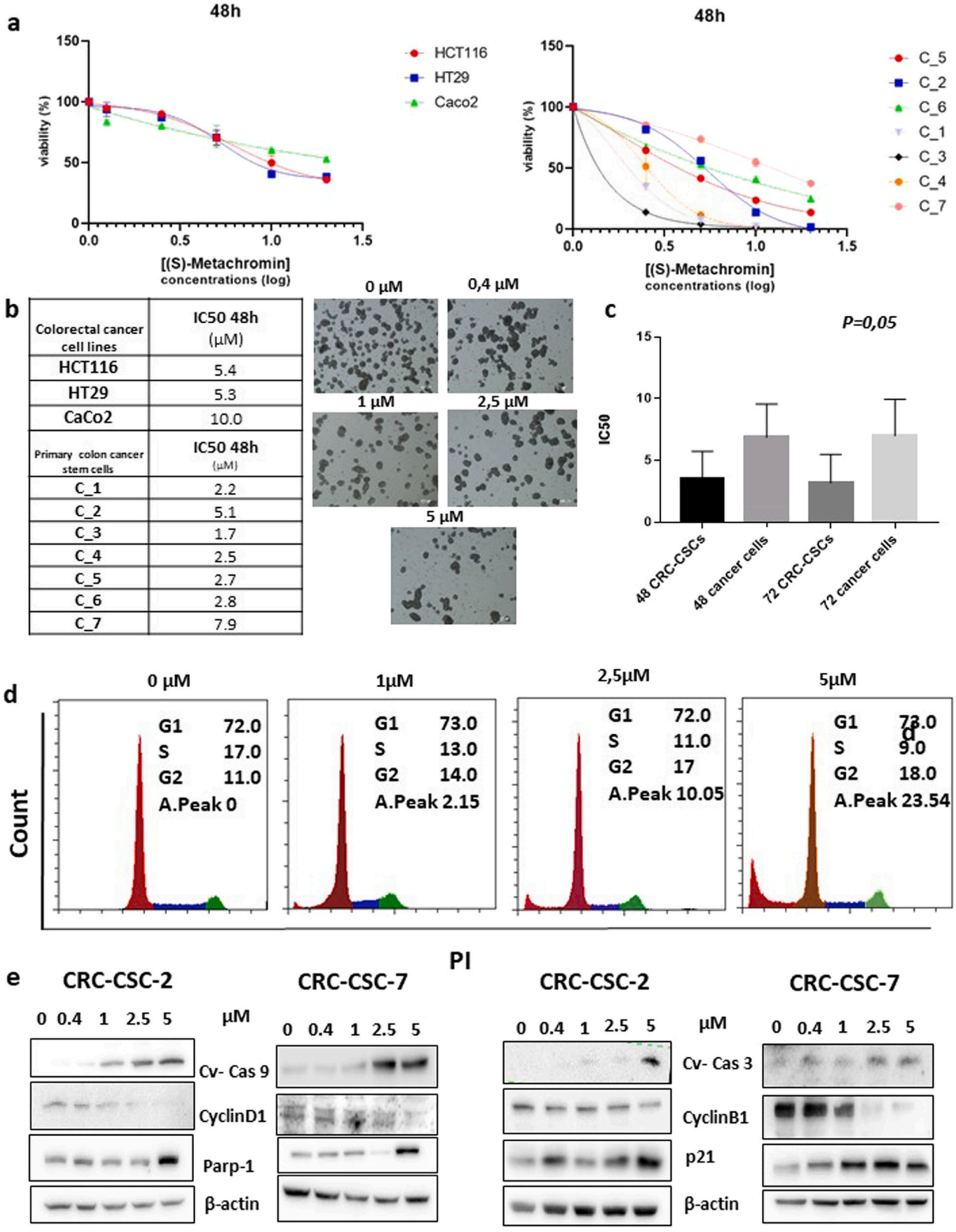

Colorectal cancer cell lines	IC50 48h (µM)
HCT116	5.4
HT29	5.3
CaCo2	10.0
Primary colon cancer stem cells	**IC50 48h (µM)**
C_1	2.2
C_2	5.1
C_3	1.7
C_4	2.5
C_5	2.7
C_6	2.8
C_7	7.9

Fig. 1. S-MV inhibits proliferation and induces apoptosis of CRC-CSCs. a-b-c) impact on cell viability of growing doses of S-MV in CRC-CSC (from C_1 to C_7) and iCCL (HCT116, CaCo2, HT29) at 48 h. C_1 and C_2: KRAS wt and BRAF wt; C_3, C_7 and C_4: Kras mut and BRAF wt; C_5 and C_6: Kras wt and BRAF mut. d) S-MV strongly affected cell cycle progression, in a dose dependent manner, causing a reduction in of cells in the G1/S and a substantial increase in the G2 cell cycle phases, along with accumulation of the sub-G0 fraction, indicative of apoptosis. e) Expression of master regulators of cell cycle and apoptosis (cyclins B1, D1, the CDK inhibitor p21Waf1, Parp-1, Caspase-3 and Caspase-9) in CRC-CSCs after S-MV treatment.

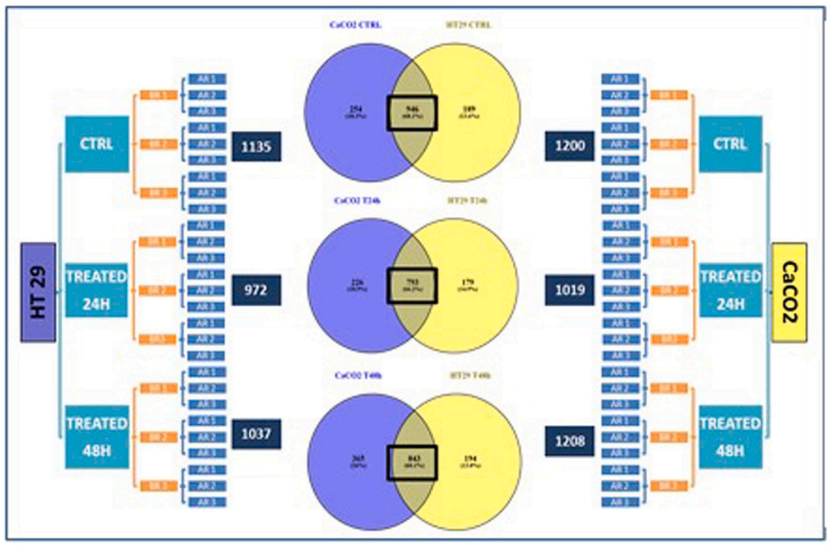

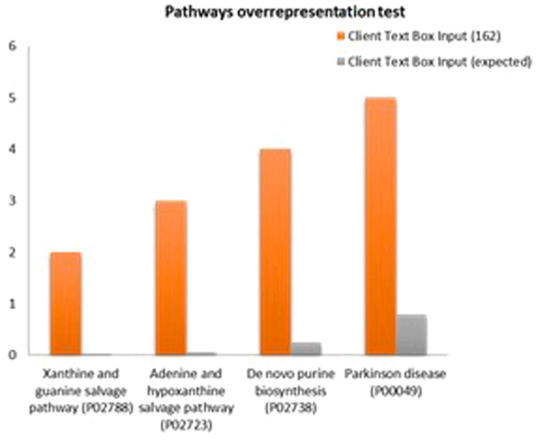

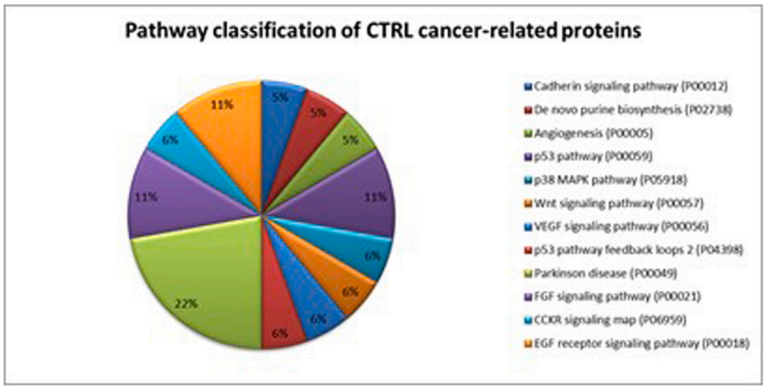

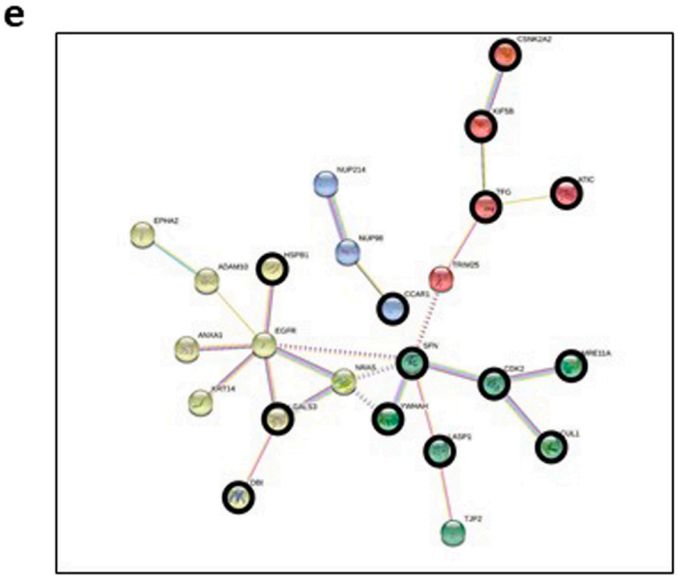

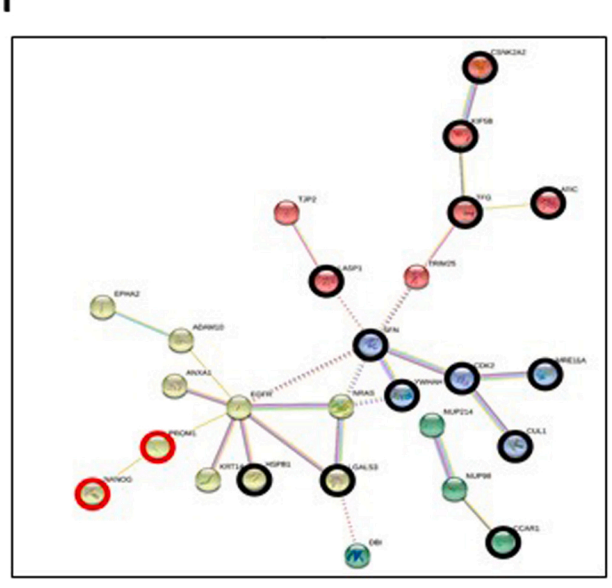

(caption on next page)

Fig. 2. Proteomic analysis on colon cancer cells treated with S-MV. a) Workflow of proteomic analysis of HT29 and CaCO2 cell lines under 24 h and 48 h treatment with S-MV. The boxes mark the number of protein elements commonly identified in both cell lines under the different conditions of untreated (CTRL) and treated (TREATED 24 h and TREATED 48 h) cells; b) grouping analysis of the CTRL and 24 h and 48 h common proteins in the box in panel a; c) results of the pathway over-representation analysis of the 162 proteins resulted exclusive of CTRL; d) grouping analysis, as in panel b, although limited to the extracted list of cancer-related classified proteins; e) protein-protein functional interaction network of the cancer-related proteins identified as exclusive of the different cell treatments and reported in Table S1 obtained by STRING tool analysis in high confidence (disconnected nodes hidden) (underlined in black the CTRL exclusive cancer-related proteins connected to the network); f) the same analysis as in panel e performed by including the Homeobox protein NANOG (NANOG) and CD133 (prominin-1, PROM1) as external interacting nodes (underlined in red).

the two cell lines. The analysis of the cell lysates after 24 h treatment (T 24 h) with S-MV resulted in 972 and 1019 proteins identified in HT29 and CaCo2 cells, respectively, 793 in common between the two cell lines. The analysis of the cell lysates after 48 h treatment (T 48 h) resulted in 1037 and 1208 proteins identified, 843 in common between the two cell lines. The attention was then focused on the elements that commonly characterized each condition in both cell lines (Fig. 2a, boxed values) to discover, by Venn diagram elaboration (Fig. 2b), the relative exclusive proteins and to evaluate the effects of S-MV action from a proteomic perspective.

The first effect emerging was the different modulation of the proteome occurring at different times of S-MV administration (Fig. 2b). In fact, despite the 41 protein elements equally modulated at all times, 28 and 47 proteins resulted exclusively identified after 24 h and 48 h of S-MV administration, respectively. The attention was at first focused on the elements that exclusively characterized the different conditions to disclose the molecular processes possibly turned off and turned on in cancer cells as a result of the S-MV activity. The 162 elements exclusive of CTRL were the first group examined, since they possibly include the protein targets of the S-MV action. Their pathways over-representation analysis by Fisher test type with FDR correction by PANTHER tool showed the over-representation of the Xanthine and guanine salvage, adenine and hypoxanthine salvage, de novo purine biosynthesis and Parkinson disease pathways with fold increase of 63.5, 54.5, 16.4 and 6.3, respectively, compared to *Homo sapiens* whole genome reference list (Fig. 2c). On the opposite, the pathway overrepresentation analysis of the proteins exclusive of treated cells did not evidence pathways over-represented. This could be indicative of pseudo-normal conditions restored following S-MV administration. We next extracted from these lists the proteins classified as cancer-related, based on Human Protein Atlas database classification. Fig. 2c shows the results from their grouping analysis and Supp. Table 1 describes the group of cancer-related proteins exclusive of each condition. The 24 cancer-related proteins exclusive of CTRL were classified in twelve pathways (Fig. 2d), with the 22 % enclosed in the Parkinson disease pathway, while the 11 % in the FGF signaling, p53 and Wnt signaling pathways, in accordance with the results of pathways overrepresentation analysis previously illustrated (Fig. 2c).

Protein-protein functional interaction network analysis by STRING tool provided evidence, by high confidence analysis, of the potential relationships between the cancer-related proteins listed in Supp. Table 1, showing interacting nodes and selected clusters (Fig. 2e). In the figure the CTRL exclusive cancer-related proteins, that could be potential targets of S-MV, are underlined in black. The network displayed significantly more interactions than expected showing the Cell cycle KEGG pathway and 12 Reactome pathways as significantly enriched, namely, the Cell Cycle, Innate Immune System, Immune System, Membrane Trafficking, Transcriptional Regulation by TP53, Neutrophil degranulation, Gene expression (Transcription), Signaling by EGFR, EGFR Transactivation by Gastrin, G2/M Checkpoints, Cell Cycle Checkpoints, Signaling by PTK6 pathways (Supp. Table 2). STRING analysis was than performed this time including both the Homeobox protein NANOG (NANOG) and CD133 (prominin-1, PROM1), considered CRC-CSC markers, as external interacting nodes (Fig. 2f). Interestingly, NANOG and PROM1 resulted functionally connected to the main protein cluster through EGFR. Among the clusters, the Cell Cycle and Apoptosis Regulator (CCRA1) protein was identified as potential target due to the relationship with CSC phenotype [21]. In this network, the KEGG Cell Cycle pathways resulted again significantly enriched together with Immune system pathways classified by Reactome.

3.4. Treatment with S-MV affects stemness and motility features in CRC cancer cells

Functional and proteomic data suggested possible effects of S-MV on cancer stem cells features. For this reason, CRC CSCs were treated with growing doses of S-MV and the expression of specific proteins was evaluated by western blot. As shown in Fig. 3a, S-MV significantly reduced the levels of stemness markers such as CD133, SOX2 and NANOG in CRC-CSCs (#2 and #7). Aberrant activation of the Wnt/β-catenin signaling pathway is implicated in growth-associated diseases and cancers, especially as a key driver in CRC initiation and progression. Based on the proteomic data showing a potential alteration of Wnt signaling pathway upon S-MV treatment, we analyzed Beta-Catenin and C-Myc expression (both related also to CD44) by western blot. We observed an overall decrease of this pathway, associated with a reduction in the activity of the Akt-Erk axys (Fig. 3a; Supp. Fig. 1c). We next verified whether the reduction of these proteins led to functional loss of stemness/aggressive traits in CRC-CSCs. We observed that S-MV impaired cancer cells' migration in a dose-dependent manner, up to 80 % (Fig. 3b-c; Supp. Fig. 2a). Cell motility is regulated, in large part, by the controlled assembly and disassembly of the actin cytoskeleton. To verify whether S-MV might also affect actin cytoskeleton assembly, we used confocal microscopy to assess the polarization of cell structure, measured as actin fiber coherency in CRC-CSCs. Motile cells must assemble their cytoskeletal actin filaments in a spatially organized way, such that net filament growth and cell protrusion occur at the front of the cell. The coherency is calculated from the structure tensor of each pixel in the images and is bounded between 0 (isotropic areas) and 1 (highly oriented structures). We found that S-MV induced an important reorganization of actin filaments with decreased coherency indicating a lower organization of cytoskeleton compared with control cells (Fig. 3c, Supp. Fig. 2b). Accordingly, expression levels of Rho GTPases (RhoA, Rac1, Cdc42) well-known modulators of cells motility, were affected by treatment with S-MV (Fig. 3d; Supp. Fig. 2c).

3.5. CCAR1 as potential target of S-MV

CCAR1 is a cancer related protein that has emerged as key player in physiology and pathophysiology, with critical roles in the DNA damage response, nuclear receptor function, Wnt signaling, and cancer stemness [24]. Since our data showed a modulation of the Wnt/beta catenin pathway as well as a reduction of the CD133, Nanog and SOX2 expression, we decided to validate our proteomic data by analyzing the expression of CCAR1. As expected, CCAR1 expression strongly decreased after S-MV treatment in all CRC tested (Fig. 4a). Moreover, using DDK1, a secreted inhibitor of beta-catenin-dependent Wnt signaling, we confirmed that the expression of CCAR1 is related to Wnt/beta catenin pathway. Indeed, DKK1 treatment induced a dose-dependent inhibition of CCAR1 in HT29 cells (Fig. 4c).

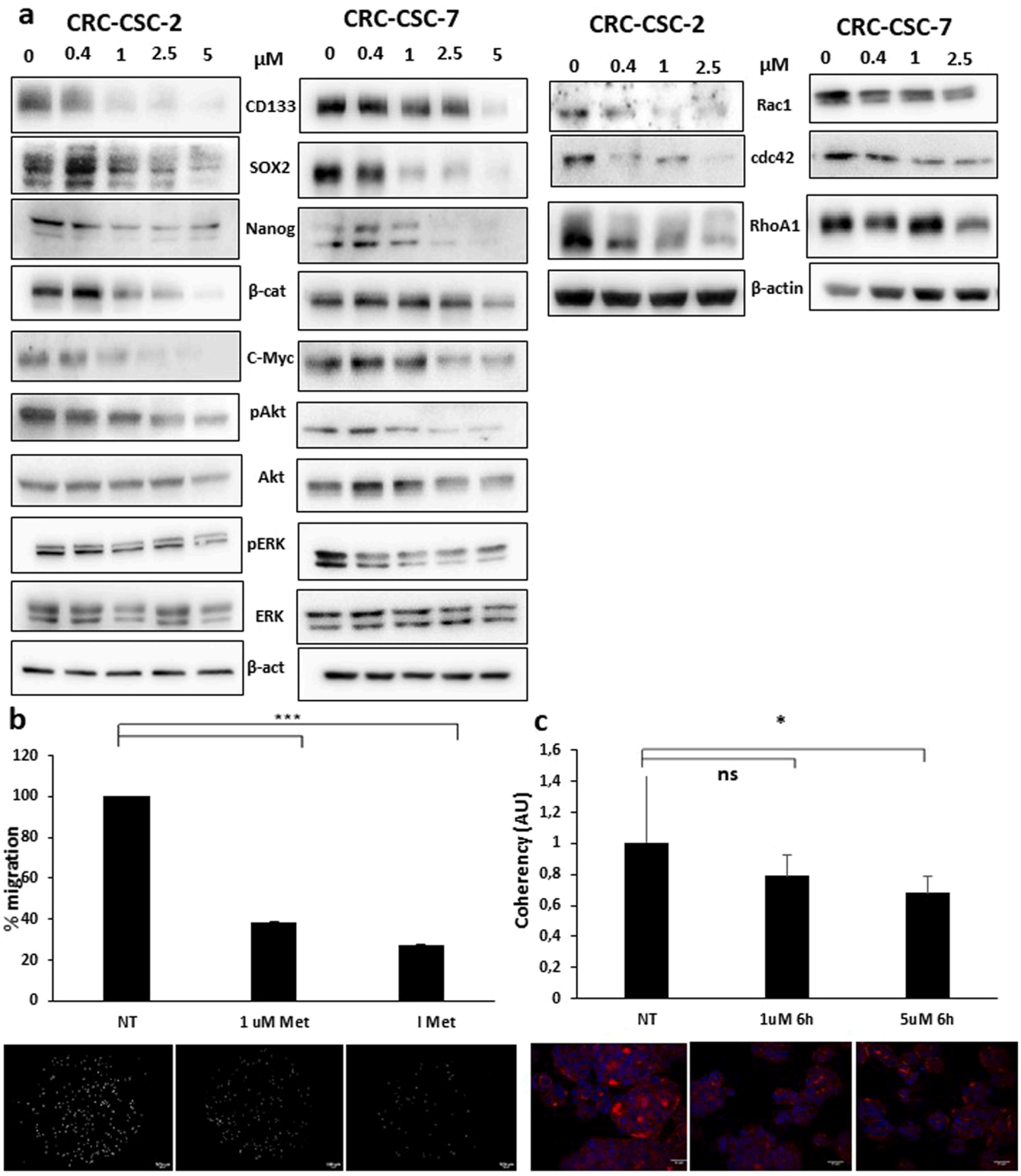

Fig. 3. Treatment with S-MV affects stemness and motility features in CRC cancer cells. a) Expression of stemness markers (CD133, Sox2 and Nanog) in CRC-CSCs (#2 and #7) and proteins involved in the Wnt/β-catenin signaling pathway (C-Myc, Akt, pAkt, Erk, pErk); b) Migration evaluation of CRC-CSCs treated with S-MV that showed an impaired cancer cells' migration; c) Actin organization after S-MV in CRC-CSCs cells. The coherency is calculated from the structure tensor of each pixel in the images and is bounded between 0 (isotropic areas) and 1 (highly oriented structures). d) Evaluation of RhoGTPase expression (RhoA, Rac1, CdC42) related to cell motility and reorganization of cytoskeleton. $p \leq 0.05$; ***, $p \leq 0.0001$.

3.6. S-MV exerts anti-tumor properties on metastatic chemo-resistant primary cells

To further understand the clinical relevance of these findings, we challenged our collection of CRC-CSC derived from CRC liver metastases (mCRC-CSCs). Metastatic patients are commonly treated with conventional chemotherapy before they undergo hepatic resection and they can be classified as responsive or resistant based on pre-operative

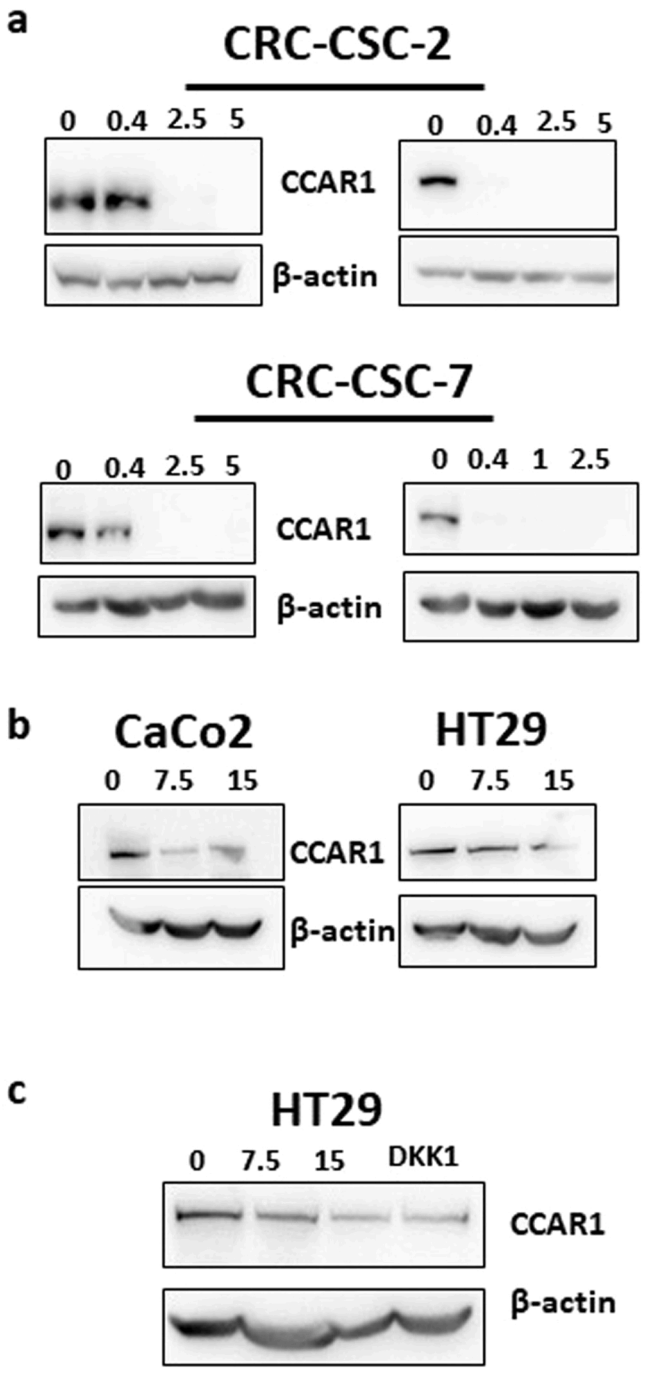

Fig. 4. CCAR1 as potential target of S-MV.a, b) Evaluation of CCAR1 expression that strongly decreased after S-MV treatment in all CRC tested (#2, #7, HT29, HCT116, CaCo2). **c)** DDK1 (Wnt inhibitor) treatment confirm the decrease of CCAR1 expression in HT29 cell line.

evaluations (partial response: RESPONSIVE; no response or progression: RESISTANT). We tested the effect of S-MV on the viability/proliferation of mCSCs derived from patients resistant to therapy. These cells retain in vitro the features of the patient of origin and reproduce the resistance to 5-Fluoro Uracile combined with Oxaliplatin (FOX) (Fig. 5, Supp. Fig. 3 and data not shown). We observed a strong impact of S-MV on the viability of chemo-resistant mCSCs derived from 4 patients, even though at higher doses if compared with CSCs isolated from naïve primary tumors (mean IC_{50} at 48 h 6,7 uM; mean IC_{50} at 6,9 uM). These promising results suggest a possible exploitation of S-MV in the clinical management of those patients that are not responding to conventional treatment.

4. Discussion

Treatment of CRC patients depends on tumor staging and Fluorouracil (5- FU)-based therapy is generally the first-line systemic approach used, in combined regimens with oxaliplatin or irinotecan. Although the combination of these drugs with targeted therapies hitting specific oncogenic pathways and/or pro-angiogenic factors has improved the overall survival, the therapeutic efficacy is hampered by undesired toxicity and CRC recurrence. Cancer stem cells (CSC) play a key role in standard treatment resistance and tumor recurrence. Hence, the development of new approaches able to tackle both the toxicity issues of chemotherapy and the resistance of CSCs is of primary relevance.

Several FDA-approved anticancer drugs are natural compounds. The alkaloids vincristine and vinblastine are used as first-line therapy for leukemia and lymphomas while paclitaxel is the first-line therapy for breast cancer. Of note, irinotecan is a drug developed from the alkaloid camptothecin and leucovorin (folinic acid) is administered together with 5FU to increase the efficacy of chemotherapy while reducing the side effects.

In our study, we evaluated the efficacy of S-MV as an anticancer drug on CRC cells. Particularly, we tested S-MV activity on colon CSCs as well on immortalized CRC cell lines. While the anticancer activity of natural [25,26] and natural-derived [27] meroterpenoids has been previously explored, less extensive is the literature specifically regarding the therapeutic potential of prenyl- quinone/hydroquinones meroterpenes, structurally related to S-MV [13,28]. The anticancer activity of S-MV towards CRC cells is probably exerted in a pleiotropic way, modulating different cell biochemical pathways, through different mechanisms thus giving rise to multiple biological effects, a common feature of other anticancer NPs [8].

Here, we exploited a collection of patient-derived CSCs, as well as immortalized CRC cells, to test and characterize the anti-cancer properties of S-MV. Firstly, we observed that S-MV strongly affects cell cycle progression due to a block in G2 phase, showing a similar overall effect in all the cell lines tested (more pronouncedly in CRC-CSCs than in immortalized cells). Further, S-MV induced an important reorganization of the cytoskeleton, as confirmed by the alterations in the expression levels of Rho GTPases (RhoA, Rac1, CDC42), leading to a reduced motility and invasion ability of cells (Fig. 5d). Finally, S-MV treatment was able to induce apoptosis, even in therapy resistant CSCs. Consistently with these phenotypes, we observed an overall downregulation of stemness markers, such as Wnt/b Catenin, Sox2, Nanog and CD133, in S-MV treated cells.

Proteomic analyses provided hints on the possible mechanism(s) of action of S-MV. Specifically, we focused on the role of CCAR1 as a possible direct target of S-MV. A plausible connection between these two biological events emerged from the proteomic analysis which highlighted the involvement of CCAR1 subsequently confirmed also by western blots. CARP-1/CCAR1 regulates apoptosis under stress conditions, such as during chemotherapy treatments [29], inducing, consistent with our findings, a decreased expression of cyclin B, C-Myc and an enhanced presence of CASP-3, 6 [29]. CARP- 1/CCAR1 was also found to be a binding partner of β-catenin enhancing the transcriptional activation of β-catenin-Wnt target genes [29]. In a recent study, it was shown to mediate anchorage independent growth of CRC cells with suppression of CARP-1/CCAR1 being able to reduce the ability of CRC to form colonies in soft agar [24,29], in accordance with our findings (Fig. S4 A).

From a mechanistic point of view, not much data is available on the structure-activity relationship of Metachromin V. If we focus on the two main structural features of the molecule, the part of the cyclohexene part which includes the prenyl moiety, looks like a shortened version of All Trans Retinoic Acid (ATRA) which inhibits the proliferation of CRC cells [30]. Interestingly, the 3-farnesyl-2-hydroxy-5-methoxy quinone from *Verongula rigida* sponge, structurally correlated to S-MV but lacking the

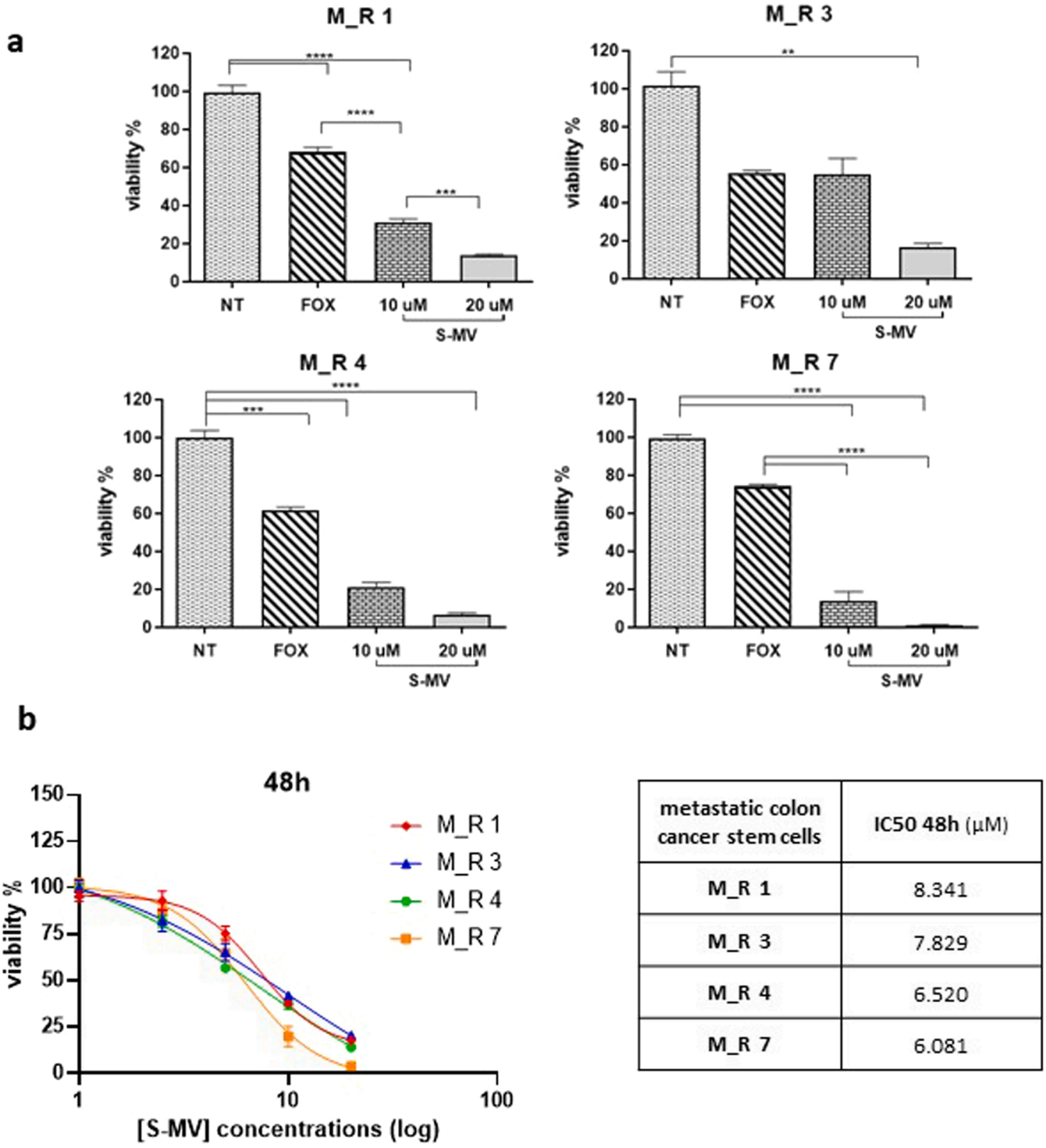

metastatic colon cancer stem cells	IC50 48h (μM)
M_R 1	8.341
M_R 3	7.829
M_R 4	6.520
M_R 7	6.081

Fig. 5. Chemo-resistant mCRC-CSCs are sensitive to S-MV. a) mCRC-CSCs isolated from liver metastasis of patients NOT responding to therapy were treated with standard chemotherapy (FOX: 5FU+OXALIPLATIN 10 mM) and different doses of S-MV for 72 h. Cell viability was measured by Cell Titer Glo (Promega). b) The same mCRC-CSCs were treated with growing doses of S-MV and IC50 values were calculated. The panel shows dose response curves after 48 h of S-MV treatment at concentrations between 2,5 and 20 μM. Values are normalized to vehicle-treated cells (DMSO). The IC50 are indicated in the table.

cyclohexane moiety, showed a complete lack of cytotoxicity towards the HCT116 CRC cell line [31].

On the other hand, Metachromin X and Y, structurally closely related to S-MV, showed a similar effect on HeLa/Fucci2 cells by blocking their cycle in S/G2/M phases [32] thus enforcing the hypothesis of the importance of the cyclohexene moiety for S-MV bioactivity. On the contrary, Jaspaquinol, a meroterpene isolated from the sponge *Jaspis splendens* [33], showed an anticancer activity against the urothelial carcinoma EJ cell line, only at 100 μM. Jaspaquinol carries a geranyl chain linking the hydroquinone and cyclohexenyl rings in the place of the prenyl chain present in S-MV. Further mechanistic studies are required to solve the exact mechanism(s) by which compounds such as S-MV act on cancer cells but based on our data and recent literature, we believe that S-MV may eventually find its way to the clinic.

5. Conclusion

We tested and confirmed S-MV anticancer activity in several CSCs isolated from primary and metastatic lesions of colorectal cancer patients and we highlighted that S-MV affects the Wnt/β-catenin signaling pathway by modulating the CCAR1 protein activity. Interestingly, the efficacy of S-MV was also confirmed on metastatic cells purified and propagated from patients resistant to therapy, thus supporting the development of this molecule as a potential aid for treatment of mCRC patients. These promising results will require further investigations to confirm the role of CCAR1 as a direct target of S-MV, to elucidate the mechanism of action of this natural compound, including also the evaluation of the R-MV enantiomer and/or of the racemic form, and to validate its efficacy in in vivo models of CRC.

CRediT authorship contribution statement

Donatella Lucchetti: Conceptualization, Methodology, Formal analysis, Data Curation, Writing - Original Draft. **Francesca Luongo**: Methodology, Formal analysis, Data Curation. **Filomena Colella**: Methodology, Formal analysis, Data Curation. **Enrico Gurreri**: Methodology, Formal analysis. **Giulia Artemi**: Methodology, Formal analysis. **Claudia Desiderio**: Methodology, Formal analysis. **Stefano Serra**: Data Curation, Formal analysis, Writing - Original Draft. **Felice Giuliante**: Writing - Review & Editing. **Ruggero De Maria**: Writing - Review & Editing. **Alessandro Sgambato**: Writing - Original Draft, Writing - Review & Editing. **Alberto Vitali**: Methodology, Formal analysis, Writing - Original Draft. **Micol Eleonora Fiori**: Conceptualization, Formal analysis, Writing - Original Draft.

Declaration of Competing Interest

We wish to confirm that there are no known conflicts of interest associated with this publication and there has been no significant financial support for this work that could have influenced its outcome.

Appendix A. Supporting information

Supplementary data associated with this article can be found in the online version at doi:10.1016/j.biopha.2023.114679.

References

[1] F. Bray, J. Ferlay, I. Soerjomataram, R.L. Siegel, L.A. Torre, A. Jemal, Global cancer statistics 2018: GLOBOCAN estimates of incidence and mortality worldwide for 36 cancers in 185 countries, CA Cancer J. Clin. 68 (6) (2018) 394–424 (Nov).

[2] K.K. Ciombor, C. Wu, R.M. Goldberg, Recent therapeutic advances in the treatment of colorectal cancer, Annu Rev. Med. 66 (2015) 83–95.

[3] A. Sartore-Bianchi, L. Trusolino, C. Martino, K. Bencardino, S. Lonardi, F. Bergamo, V. Zagonel, F. Leone, I. Depetris, E. Martinelli, T. Troiani, F. Ciardiello, P. Racca, A. Bertotti, G. Siravegna, V. Torri, A. Amatu, S. Ghezzi, G. Marrapese, L. Palmeri, E. Valtorta, A. Cassingena, C. Lauricella, A. Vanzulli, D. Regge, S. Veronese, P. M. Comoglio, A. Bardelli, S. Marsoni, S. Siena, Dual-targeted therapy with trastuzumab and lapatinib in treatment-refractory, KRAS codon 12/13 wild-type, HER2-positive metastatic colorectal cancer (HERACLES): a proof-of-concept, multicentre, open-label, phase 2 trial, Lancet Oncol. 17 (6) (2016) 738–746 (Jun).

[4] L. Ricci-Vitiani, D.G. Lombardi, E. Pilozzi, M. Biffoni, M. Todaro, C. Peschle, De, R. Maria, Identification and expansion of human colon-cancer-initiating cells, Nature 445 (7123) (2007) 111–115. Jan 4.

[5] K.K. Ciombor, C. Wu, R.M. Goldberg, Recent therapeutic advances in the treatment of colorectal cancer, Annu Rev. Med. 66 (2015) 83–95.

[6] J.W. Blunt, B.R. Copp, R.A. Keyzers, M.H. Munro, M.R. Prinsep, Marine natural products, Nat. Prod. Rep. 32 (2) (2015) 116–211 (Feb).

[7] M.F. Mehbub, J. Lei, C. Franco, W. Zhang, Marine sponge derived natural products between 2001 and 2010: trends and opportunities for discovery of bioactives, Mar. Drugs 12 (8) (2014) 4539–4577. Aug 19.

[8] C. Calcabrini, E. Catanzaro, A. Bishayee, E. Turrini, C. Fimognari, Marine sponge natural products with anticancer potential: an updated review, Mar. Drugs 15 (10) (2017) 310. Oct 13.

[9] H.J. Choi, S.J. Bae, N.D. Kim, J.H. Jung, Y.H. Choi, Induction of apoptosis by dideoxypetrosynol A, a polyacetylene from the sponge Petrosia sp., in human skin melanoma cells, Int. J. Mol. Med. 14 (6) (2004) 1091–1096.

[10] L. Fiorini, M.A. Tribalat, L. Sauvard, J. Cazareth, E. Lalli, I. Broutin, O.P. Thomas, I. Mus-Veteau, Natural paniceins from mediterranean sponge inhibit the multidrug resistance activity of Patched and increase chemotherapy efficiency on melanoma cells, Oncotarget 6 (26) (2015) 22282–22297, 8.

[11] F. Funk, K. Krüger, C. Henninger, W. Wätjen, P. Proksch, J. Thomale, G. Fritz, Spongean alkaloids protect rat kidney cells against cisplatin-induced cytotoxicity, Anticancer Drugs 25 (8) (2014) 917–929 (Sep).

[12] Bioactive Prenyl- and Terpenyl-Quinones/Hydroquinones of Marine Origin. P. A. García, Á. P. Hernández, A. San Feliciano, M. Á. Castro. Mar. Drugs 2018, 16, 292;

[13] S.P. Ovenden, J.L. Nielson, C.H. Liptrot, R.H. Willis, D.M. Tapiolas, A.D. Wright, C. A. Motti, Metachromins U-W: cytotoxic merosesquiterpenoids from an Australian specimen of the sponge Thorecta reticulata, J. Nat. Prod. 74 (5) (2011) 1335–1338. May 27.

[14] S. Serra, A.A. Cominetti, V. Lissoni, A general synthetic approach to hydroquinone meroterpenoids: stereoselective synthesis of (+)-(S)-metachromin V and alliodorol, Nat. Prod. Commun. 9 (3) (2014) 303–308.

[15] A. Calcaterra, I. D'Acquarica, The market of chiral drugs: chiral switches versus de novo enantiomerically pure compounds, J. Pharm. Biomed. Anal. 147 (2018) 323–340 (Jan 5).

[16] V.V.S.P. Kumari Rayala, J.S. Kandula, R. P, Advances and challenges in the pharmacokinetics and bioanalysis of chiral drugs, Chirality (2022).

[17] M.M. Coelho, C. Fernandes, F. Remião, M.E. Tiritan, Enantioselectivity in drug pharmacokinetics and toxicity: pharmacological relevance and analytical methods, Molecules 26 (11) (2021) 3113 (May 23).

[18] J.L. Fischel, P. Formento, J. Ciccolini, P. Rostagno, M.C. Etienne, J. Catalin, G. Milano, Impact of the oxaliplatin-5 fluorouracil-folinic acid combination on respective intracellular determinants of drug activity, Br. J. Cancer 86 (2002) 1162–1168.

[19] J.R. Wiśniewski, A. Zougman, N. Nagaraj, M. Mann, Universal sample preparation method for proteome analysis, Nat. Methods 6 (5) (2009) 359–362 (May).

[20] E.W. Deutsch, C.M. Overall, J.E. Van Eyk, M.S. Baker, Y.K. Paik, S.T. Weintraub, L. Lane, L. Martens, Y. Vandenbrouck, U. Kusebauch, W.S. Hancock, H. Hermjakob, R. Aebersold, R.L. Moritz, G.S. Omenn, Human proteome project mass spectrometry data interpretation guidelines 2.1, J. Proteome Res. 15 (11) (2016) 3961–3970. Nov 4.

[21] Huaiyu Mi, Dustin Ebert, Anushya Muruganujan, Caitlin Mills, Laurent-Philippe Albou, Tremayne Mushayamaha, Paul D Thomas, PANTHER version 16: a revised family classification, tree-based classification tool, enhancer regions and extensive API, Nucl. Acids Res. (2020).

[22] D. Szklarczyk, A.L. Gable, D. Lyon, A. Junge, S. Wyder, J. Huerta-Cepas, M. Simonovic, N.T. Doncheva, J.H. Morris, P. Bork, STRING v11: protein–protein association networks with increased coverage, supporting functional discovery in genome-wide experimental datasets, Nucleic Acids Res. 47 (2019) D607–D613.

[23] M. Uhlen, C. Zhang, S. Lee, E. Sjöstedt, L. Fagerberg, G. Bidkhori, R. Benfeitas, M. Arif, Z. Liu, F. Edfors, K. Sanli, K. von Feilitzen, P. Oksvold, E. Lundberg, S. Hober, P. Nilsson, J. Mattsson, J.M. Schwenk, H. Brunnström, B. Glimelius, T. Sjöblom, P.H. Edqvist, D. Djureinovic, P. Micke, C. Lindskog, A. Mardinoglu, F. Ponten, A pathology atlas of the human cancer transcriptome, Science 357 (6352) (2017), eaan2507.

[24] L. Wang, L. Zhao, Z. Lin, D. Yu, M. Jin, P. Zhou, J. Ren, J. Cheng, K. Yang, G. Wu, T. Zhang, D. Zhang, Targeting DCLK1 overcomes 5-fluorouracil resistance in colorectal cancer through inhibiting CCAR1/β-catenin pathway-mediated cancer stemness, Clin. Transl. Med. 12 (5) (2022), e743.

[25] J.E. Kim, J.H. Kim, Y. Lee, H. Yang, Y.S. Heo, A.M. Bode, K.W. Lee, Z. Dong, Bakuchiol suppresses proliferation of skin cancer cells by directly targeting Hck, Blk, and p38 MAP kinase, Oncotarget 7 (12) (2016) 14616–14627.

[26] M. Gordaliza, Cytotoxic terpene quinones from marine sponges, Mar. Drugs 8 (12) (2010) 2849–2870, https://doi.org/10.3390/md8122849.

[27] C. Imperatore, G. Della Sala, M. Casertano, P. Luciano, A. Aiello, I. Laurenzana, C. Piccoli, M. Menna, In vitro antiproliferative evaluation of synthetic meroterpenes inspired by marine natural products, Mar. Drugs 17 (12) (2019) 684.

[28] J. Kobayashi, T. Murayama, Y. Ohizumi, T. Ohta, S. Nozoe, T. Sasaki, Metachromin C a new cytotoxic sesquiterpenoid from the Okinawan marine sponge Hippospongia metachromia, J. Nat. Prod. 52 (5) (1989) 1173–1177.

[29] M. Muthu, V.T. Cheriyan, A.K. Rishi, CARP-1/CCAR1: a biphasic regulator of cancer cell growth and apoptosis, Oncotarget 6 (9) (2015) 6499–6510.

[30] Weihong Liu, Yanqiu Song, Chenggui Zhang, Pengfei Gao, Bisheng Huang, Jianfang Yang, The protective role of all-transretinoic acid (ATRA) against colorectal cancer development is achieved via increasing miR-3666 expression and decreasing E2F7 expression, Biomed. Pharmacother. 104 (2018) 94–101.

[31] A. Jiso, P. Demuth, M. Bachowsky, M. Haas, N. Seiwert, D. Heylmann, B. Rasenberger, M. Christmann, L. Dietrich, T. Brunner, et al., Natural merosesquiterpenes activate the DNA damage response via DNA strand break formation and trigger apoptotic cell death in p53-wild-type and mutant colorectal cancer, Cancers 13 (2021) 3282.

[32] Y. Hitora, K. Takada, Y. Ise, S.P. Woo, S. Inoue, N. Mori, H. Takikawa, S. Nakamukai, S. Okada, S. Matsunaga, Metachromins x and y from a marine sponge spongia sp. And their effects on cell cycle progression, Bioorg. Med. Chem. 28 (2020), 115233.

[33] A. Demotie, I.J. Fairlamb, F.J. Lu, N.J. Shaw, P.A. Spencer, J. Southgate, Synthesis of jaspaquinol and effect on viability of normal and malignant bladder epithelial cell lines, Bioorg. Med. Chem. Lett. 14 (11) (2004) 2883–2887.